Contributed paper

OPTO-ELECTRONICS REVIEW **11**(4), 269–275 (2003)

Industrial technology of multicrystalline silicon solar cells

P. PANEK[1*], M. LIPINSKI[1], E. BELTOWSKA-LEHMAN[1],
K. DRABCZYK[2] and R. CIACH[1]

[1]Polish Academy of Sciences, Institute of Metallurgy and Materials Science,
25 Reymonta Str., 30-059 Cracow, Poland
[2]Silesian Technical University, Institute of Electronics,
16 Akademicka Str., 44-100 Gliwice, Poland

This paper presents current technology used to produce 100 cm² multicrystalline silicon solar cells of efficiency above 13% which was one of the main goals of the National Photovoltaic Project undertaken in the Institute of Metallurgy and Materials Science (IMMS). The general concept of the technology consists of maximum seven steps. The process sequence is based on diffusion from $POCl_3$ and screen printed contacts fired through a PECVD Si_xN_y or TiO_x antireflection coating (ARC). Co-metallisation annealing was performed in an IR furnace. The multicrystalline wafers are described using four-point probe, scanning electron microscopy (SEM), secondary ion mass spectrometer, and spectrophotometer with an integrating sphere. The completed solar cells are characterized with internal spectral response and a current-voltage characteristic. All aspects playing a role in a suitable manufacturing process are discussed. At present, multicrystalline silicon solar cells capture around a 45% share of the world photovoltaics market with a total of 540 MW being produced in 2002. Taking into account the decreasing cost of multicrystalline substrates, this relation will rise systematically.

Keywords: solar cells, multicrystalline silicon, industrial technology.

1. Introduction

The industrial technology of multicrystalline silicon solar cells has been developed using the BAYSIX silicon produced by Bayer (Germany) as the base and material characterised by the following technical data: multicrystalline silicon, p-type, boron-doped, thickness ~330 μm, area 10×10 cm, resistivity ~1 Ω cm, minority carriers diffusion length ~80 μm, oxygen concentration < 5×10^{17} atom/cm^3, carbon concentration < 1×10^{18} atom/cm^3.

The diffusion length of minority carriers is the value which determines the maximum efficiency of solar cells [1]. This silicon is appropriate only for screen printing technology and has influenced elaboration focusing and a method. The final baseline process for the fabrication sequence of multicrystalline solar cells is shown in Fig. 1.

When using TiO_x as ARC, the seven main technological steps are needed or only six steps when Si_xN_y is employed.

2. Chemical preparation of the multicrystalline wafers

Different etching and cleaning techniques are necessary for preparing "as cut" silicon wafers delivered from the manufacturer. As a result of cutting wafers from a multicrystalline ingot, approximately 5 μm of material on both sides of the wafer is highly distorted and must be removed. A commonly used method, chemical etching in KOH or NaOH solution, is selective for grains with different crys-

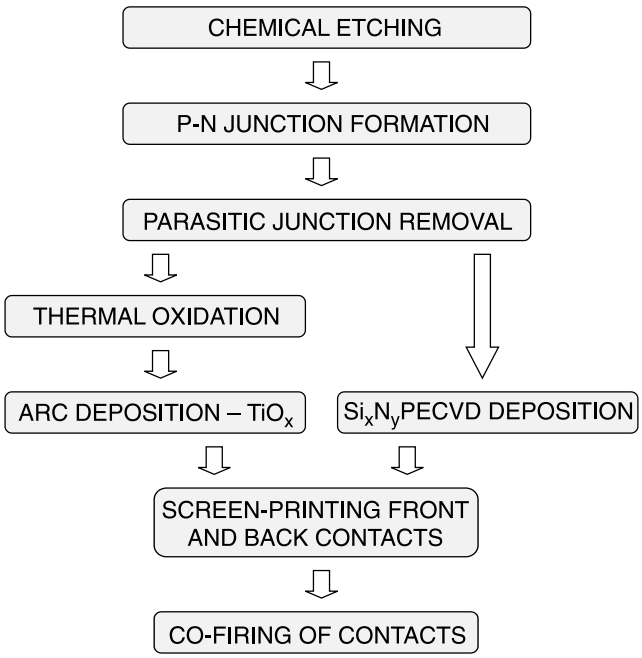

Fig. 1. Flow chart of the multicrystalline solar cells processing at IMMS PASs.

*e-mail: pan-kozy@wp.pl

Table 1. Chemical processing applied to "as-cut" silicon wafers.

Chemical process	Chemical recipe	Time (min)	Temperature (°C)
Distorted layer removing	30% KOH	15	80
Rinsing	DIH_2O	25	25
Rinsing	IPA	15	25
Texturisation	IPA : 40%KOH : DIH_2O in vol. ratio 3:1:46	15	80
Rinsing	DIH_2O	25	25
Neutralisation of potassium traces and metallic contamination removing	95% H_2SO_4 : H_2O in vol. ratio 1:1	15	25
Rinsing	DIH_2O	25	25
Metallic contamination removing	2% HCl	15	25
Rinsing	DIH_2O	25	25
Native oxide removing	10% HF	2	25
Rinsing	DIH_2O	25	25

tallographic orientation on the surface and this causes discontinuities at the grain boundaries. However, this texturisation enhanced the light absorption but not to the same extent as in the case of (100) monocrystalline silicon. Some other proposals such as laser scribing, mechanical V-grooving or reactive ion etching (RIE) cannot be easy implemented in an industrial process which needs primarily high throughput at low cost. The acid etching, being an isotropic method, is still under investigation [2,3]. The well-prepared surfaces of the wafers must, as far as possible, be free of contaminants K^+ ions from the etching solution, heavy metals and organic impurities. The chemical procedure for cleaning the wafers before the donor doping process is given in Table 1.

Following the etching and cleaning processes, the wafers were rinsed with 18 MΩ cm deionised water DIH_2O in a cascade system as the final stage. During chemical treatment, the wafers were placed in a Teflon holder which could contain 25 slices.

3. The p-n junction formation

Emitter diffusion is one of the crucial steps in the manufacturing process of silicon solar cells. The donor source can be applied by techniques such as: screen printing, spray-on, spin-on or CVD ($POCl_3$) [4]. The emitter was generated at temperatures in the range 845–890°C for 40 min. in an open quartz tube using liquid $POCl_3$ as the doping source. This results is an emitter with a sheet resistance from 20 Ω/□ to 40 Ω/□ as shown in Fig. 2. Sheet resistance was measured with automatic four-point probe which is the fundamental method used to control the diffusion process in industry. The selected wafers, measured at nine points, had emitters with homogeneity around 5% standard deviation. This is acceptable taking into account that the wafer area is 100 cm^2 and the diffusion furnace SD-3/158M has a quartz tube of 158 mm diameter. The diffusion profiles have been determined by secondary ion mass spectroscopy (SIMS) measurements.

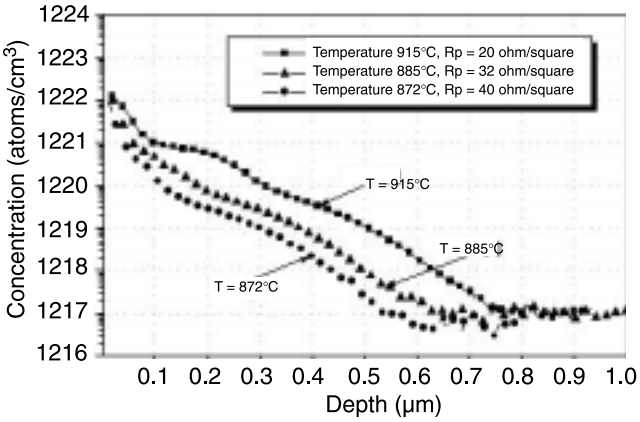

Fig. 2. Determined by SIMS phosphorous concentration profiles at diffusion time of 40 minutes in relation to diffusion temperature after process using $POCl_3$.

Table 2. The main electrical parameters of the solar cells in dependence on phosphorous concentration profile adequate to shown in Fig. 2.

Sheet resistance R_s Ω/□	I_{sc} (A)	V_{oc} (V)	FF	E_{ff} (%)
20	2.749	0.561	0.748	11.53
32	2.885	0.576	0.732	12.17
40	2.979	0.578	0.731	12.60

The cells obtained with the different emitters were analysed and, as can be seen in Table 2, the emitter with a sheet resistance in the range 40–50 Ω/□ is optimal for screen-printing technology. The form of donor doping, shown in Fig. 2, obviously depends on temperature and time, but also on the diffusion technology realised with pre-oxidation before the pre-diffusion step. The second kind of diffusion technique was the formation of a n^+/p structure using phosphorus-doped silica paste, marked by Soltech as 1. This was screen-printed onto wafers with a 220-mesh screen and after drying the wafers were placed in an IR furnace where the diffusion occurs in 5 min at a temperature above 900°C [5]. Phosphorus from paste diffuses into the desired front side of the wafer. The average results for 100 cm^2 solar cells with emitter formed with 1 paste, covered TiO_x, have reached the following value: I_{sc} = 2.589 A, V_{oc} = 0.599 V, FF = 0.74 and E_{ff} = 11.5% what is below the parameters characterised by solar cells after processing with $POCl_3$ as it can be seen in Tables 3 and 5.

4. Parasitic junction removal and chemical etching

After diffusion from $POCl_3$, the wafers are covered by phosphorus-silicate glass $xSiO_2 \cdot yP_2O_5$ and have donor-doping layer on both sides and edges. At first, the parasitic junction was removed by means of a special Teflon clamp in which the silicon wafers previously immersed in a glycerine-water solution were stacked surface by surface with EVA foil separation. Next, the clamp was immersed in 65%HNO_3:40%HF:80%CH_3COOH solution in the volume ratio 5:3:3 for 1 min. followed by rinsing in DI H_2O. Then $xSiO_2 \cdot yP_2O_5$ was removed by immersion in a bath of 10% HF for 2 min. Finishing all wet chemical baths, the wafers were dried in a spin-drier with the highly purified air. It is more difficult to obtain a clean and non-wetting wafer surface by chemical etching after using 1 paste and the phosphorus glass layer has to be removed in 25% HF using an ultrasonic cleaner.

5. Passivation process

Surface passivation was achieved by the growth of a thin, invisible passivating oxide SiO_2 at a temperature of 800°C for 15 min. in a controlled O_2 and N_2 atmosphere. Increasing the time did not increase the short circuit current I_{sc} significantly and the shorter did not give an expected improvement as it can be seen in Fig. 3 and Table 3.

The oxygen and nitrogen used for the thermal annealing and diffusion processes were dried to a dryness of 0.005 mg/l and purified with 5A Molecular Sieves system to remove impurities that have effective molecular diameter of less than 5 angstroms.

The improvement in the cell efficiency depends among others on the open circuit voltage V_{oc} and for maximising the V_{oc} it is very important to reduce the recombination velocity at the surface, under contacts and in the bulk. A thermal oxide is effective in reducing the surface recombination velocity whilst bulk passivation is possible by, for example, silicon nitride.

Table 3. The parameters current-voltage characteristic solar cells realised in technology including TiO_x as ARC with and without passivated layer SiO_2 grows for the time 15 min.

Solar cell	I_{sc} [A]	V_{oc} [V]	FF	E_{ff} [%]
Without SiO_2	2.461	0.545	0.737	9.91
With SiO_2	2.903	0.583	0.736	12.47
Change [%]	+17.9	+6.9	0	+25.8

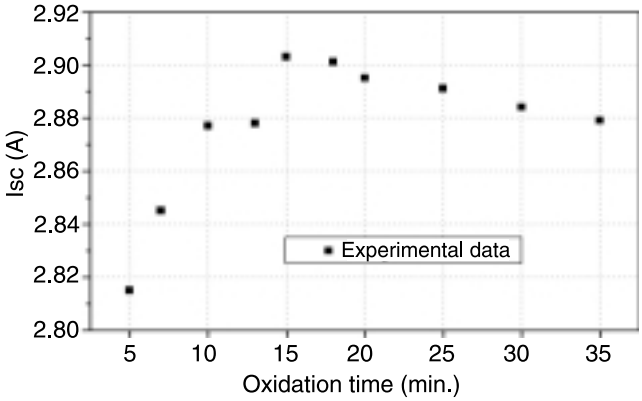

Fig. 3. Short circuit current of solar cells with TiO_x for different dry oxidation time.

6. Antireflection coatings deposition

The Si surface reflects 35–50% of the light, depending upon its wavelength in the range 400–1100 nm on which the photovoltaic conversion depends. Obtaining the lower reflective surface on the multicrystalline silicon solar cell is difficult because of the presence of randomly oriented crystallites. An improvement can be only achieved by forming an antireflection coating (ARC) to reduce the solar cell reflection to below 10% [1]. In industry two antireflection coatings are widely applied: titanium oxide TiO_x and silicon nitride Si_xN_y. Both were deposited before contacts were screen-printed. It is very important for soldering of the solar cells because before connecting them in a module there is no necessity to remove ARC from the front busbar electrode. The Si_xN_y was deposited by plasma enhanced chemical vapour deposition (PECVD). It has following advantages [6]:

- by changing the deposition conditions: power, temperature, pressure and NH_3/SiH_4 ratio Si_xN_y can be obtained with the required optical and material parameters best suited for solar cells. Specifically a refractive index of 1.9 for 600 nm wavelength, extinction coefficient above 400 nm wavelength sharply decreasing to 0, control of hydrogen content and a positive charge present on the solar cell surface,

- the Si_xN_y film deposition has a role as a bulk and surface passivator as well as providing the antireflection coating,
- it gives possibilities of simultaneous firing of front and back contacts,
- it reduces the production process to six steps as it allows the thermal oxidation process to be omitted.

The TiO_x layers have excellent optical properties as ARCs for multicrystalline solar cells. Namely, the refractive index of about 2.38 at a wavelength of 600 nm and an extinction coefficient remaining near zero under the wavelength of 400 nm [7]. A TiO_x film produced at the temperature below 300°C is primarily amorphous which makes the metallisation of the front contacts easier. According to the flow chart presented in Fig. 1, after dry passivation, the TiO_x was deposited by spraying at 280°C with tetraethylorthotitanat $(C_2H_5O)_4Ti$ using purified air as a carrier gas. Figure 4 shows internal quantum efficiency and reflectance for solar cell done with TiO_x.

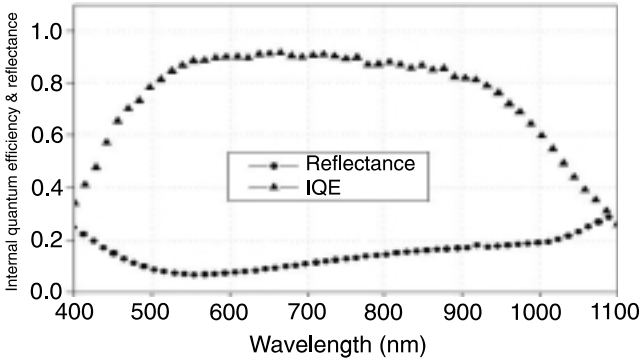

Fig. 4. Internal quantum efficiency (IQE) and reflectance for solar cell with SiO_2 passivated layer and ARC with TiO_x.

7. Screen-printing front and back contacts

The screen-printing process is very simple and commonly used in industrial production. A few types of the photovoltaic pastes were tested and eventually silver paste PV145, manufactured by Du Pont, was used on the front and aluminium T-14002A, produced by Engelhard, was used on the back and were printed using 330 mesh screens. The front paths designed on the screen were 120 μm wide with 3.3 mm spacing which gives, together with the two main collection busbars 1 mm wide, a 5.6% front shadow. Back contact covering the full rear surface was deposited with pure Al paste. The two collection back busbarr contacts were printed with a Polish silver paste P-124 containing 3% aluminium. The collection back bur contacts must not have a greater quantity of aluminium in the paste because soldering for interconnecting cells would be impossible.

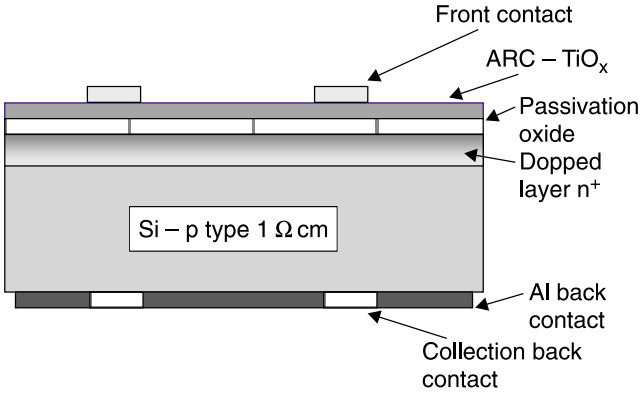

Fig. 5. Schematic structure of solar cell with TiO_x layer as ARC. If the silicon nitride is used as ARC the layer indicated as "passivation oxide" is not present.

8. Co-firing of metal contacts

A conveyor belt IR furnace with fitted tungsten filament lamps, heating the top and bottom of the belt, was used for simultaneous metallisation for the front and back electrodes [5]. The three following heating zones are 18 cm, 36 cm and 18 cm long and the belt speed is in the range 50–200 cm/min. The technical parameters of the annealing treatment are given in Table 4 while the thermal profiles are shown in Fig. 6.

After drying in air at 150°C the printed pastes were co-fired in the IR belt furnace. The wafers during metallisation are at a temperature above 577°C for about 13 seconds and obviously this process can be classified as rapid thermal annealing. This process can be qualified by the current-voltage characteristic parameters: fill factor, series and shunt resistance [1]. This IR annealing process gives an acceptable value of 10 mΩ for the series resistance and a shunt resistance of 0.035 kΩ resulting in a fill factor of 0.74.

To obtain a good back surface field (BSF) a thick aluminium layer ~20 μm is required but it cause the wafer to be bent after firing due to the different expansion coefficients of Si and Al. The degree of curvature depends on the thickness of the wafer and the 200 μm is the limit before the degree of curvature makes the cells interconnection in a

Table 4. Parameters set for the co-firing process in the IR furnace.

	I zone temperature (°C)	II zone temperature (°C)	III zone temperature (°C)	Belt speed (cm/min)
Solar cells with TiO_x	550	550	880	160
Solar cells with Si_xN_y	550	750	880	200

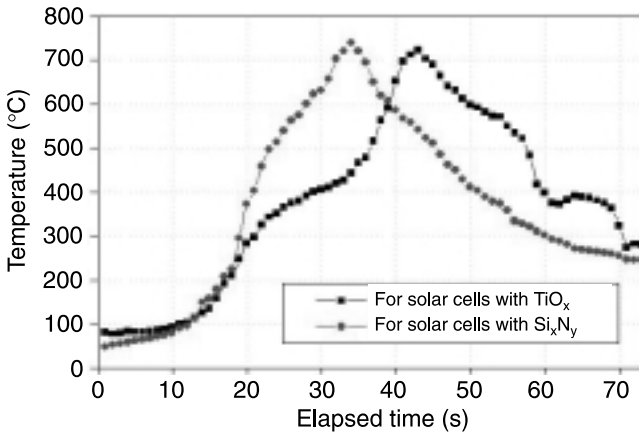

Fig. 6. Temperature profiles vs. elapsed time for solar cell metallisation in the IR furnace.

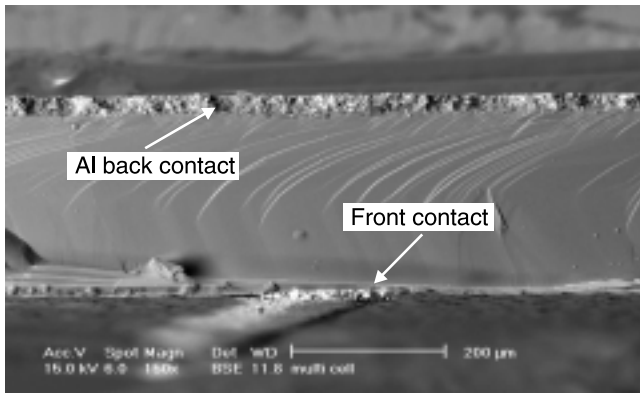

Fig. 7. SEM micrograph of cross-section multicrystalline solar cell after co-firing of metal contacts in IR furnace. The Aluminium back contact is 30-μm thick. The front electrode grid line is 160-μm wide and 25-μm high. The cell thickness is 290 μm.

standard module impossible. The Al layer not only produces a BSF but also helps to passivate defects in the bulk Si, especially when silicon nitride is applied [8].

9. Measurements and results

The illuminated I-V parameters were measured under standard simulated AM 1.5 (100 mW/cm^2) radiation and an example report is shown in Fig. 8. A reference cell was calibrated at IMEC, Belgium. To confirm the repeatability of the technology a few experimental solar cells series were produced following the procedures given in Fig. 1. Two were selected as examples; one with TiO_x and second with Si_xN_y. The results are presented in Figs. 9 and 10 showing the Gauss distribution and in Table 4.

As it can be seen good average short circuit current density, around 30 mA/cm^2, and the required photovoltaic conversion efficiency above 13% were obtained. In the case of cells with Si_xN_y, the best I_{sc} around 3.2 A and noticeable voltage 600 mV has been obtained thanks to excellent surface and bulk passivation by a hydrogenation process at temperatures of 600–800°C. An average value of 10 mΩ for the series resistance and 0.035 kΩ for the shunt re-

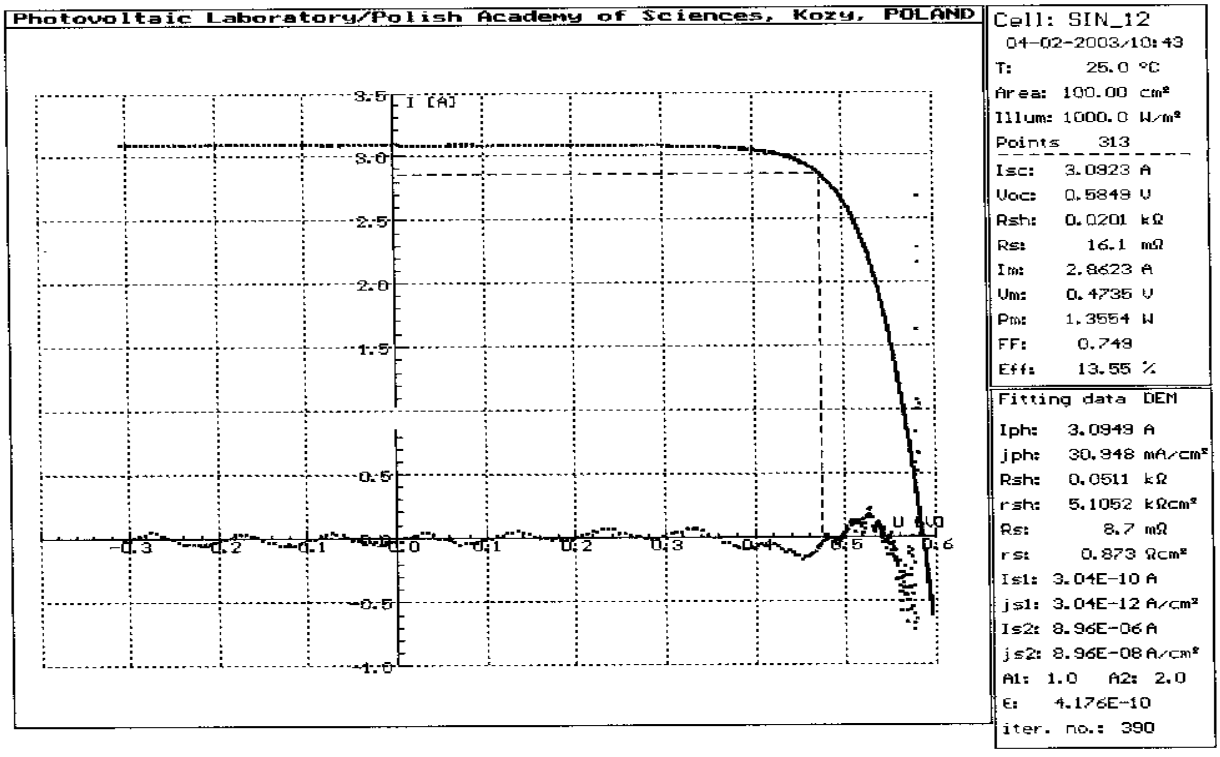

Fig. 8. The measured I-V report for multicrystalline silicon solar cell with Si_xN_y. The numerical fitting was realized by applying double exponential model containing seven modelling parameters [9].

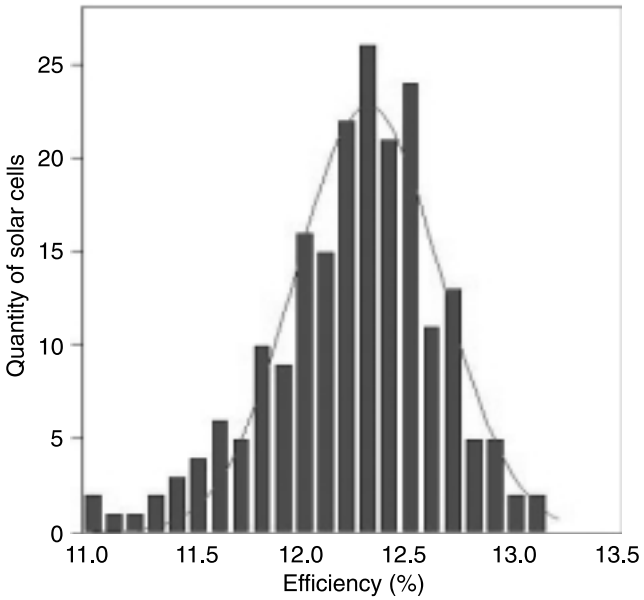

Fig. 9. Gauss distribution of efficiency for series 200 solar cells with TiO_x.

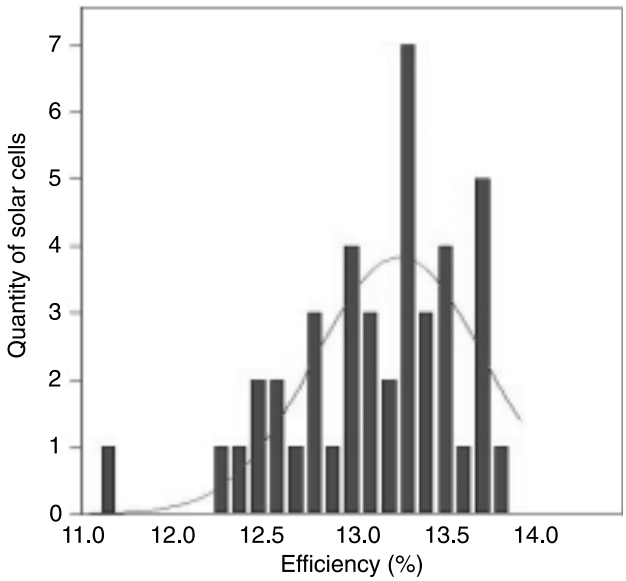

Fig. 10. Gauss distribution of efficiency for series 40 solar cells with Si_xN_y.

sistance is good and give a fill factor of 0.74. The silicon nitride allows the omission of the dry oxidation process and reduces the main fabrication steps to six. This would appear to be particularly attractive since there are no other industrial alternatives [10].

Photovoltaic cell production grew by 35% in 2002 year with a total of 540 MW being produced and multicrystalline silicon solar cells have captured around 45% of the world market [11].

10. Conclusions

- A simple industrial procedure for manufacturing high efficiency solar cells on 100-cm^2 multicrystalline silicon has been developed.
- Multicrystalline silicon solar cells with an average cell efficiency above 12% with TiO_x and 13% with Si_xN_y have been manufactured.
- The technology including TiO_x as antireflection coating can be easy transferred to a production line without incurring high costs.
- The technology for manufacturing multicrystalline silicon solar cells with Si_xN_y requires purchase of an industrial PECVD device for Si_xN_y deposition with a minimum throughput 500 silicon slices per hour. The use of this device reduced the process steps to six and opens new scientific areas.

Acknowledgements

This work was supported by the Polish State Committee for Scientific Research (KBN) under Project No. 05/T11/98. The authors would like to thank E. Bielańska from IMMS PAS in Cracow for the SEM investigation and H. Czternastek from University of Mining and Metallurgy in Cracow for reflectance measurements. We gratefully acknowledge J. Szlufcik from IMEC for his valuable contributions to this work.

Table 5. The average values calculated from Gauss distribution of the main parameters current-voltage (I-V) characteristic for 200 pieces solar cells with TiO_x and 40 pieces solar cells with Si_xN_y and the best multicrystalline 100 cm^2 solar cells in a particular series.

Average value				
	I_{sc} (A)	V_{oc} (V)	FF	E_{ff} (%)
Solar cells with TiO_x	2.960	0.575	0.722	12.29
Solar cells with Si_xN_y	3.058	0.594	0.726	13.19
Best value				
	I_{sc} (A)	V_{oc} (V)	FF	E_{ff} (%)
Solar cells with TiO_x	3.009	0.581	0.749	13.09
Solar cells with Si_xN_y	3.177	0.600	0.721	13.70

References

1. A. Goetzberger, J. Knobloch, and B. Voss, *Crystalline Silicon Solar Cells*, John Wiley & Sons, Chichester, England, 1998.
2. M. Lipinski, P. Panek, Z. Swiątek, E. Beltowska, and R. Ciach, "Double porous silicon layer on multi-crystalline Si for photovoltaic application", *Solar Energy Materials & Solar Cells* **72**, 271–276 (2002).
3. V.Y Yerokhov, M. Lipinski, R. Ciach, H. Nagel, A. Mylyanych, and P. Panek, "Cost-effective methods of texturing for silicon solar cells", *Solar Energy Materials & Solar Cells* **72**, 291–298 (2002).
4. K. Waczynski, K. Drabczyk, M. Lipinski, and P. Panek, "Doping technology using silica glasses investigation of the emitter layer of the silicon solar cell", *Proc. Int. Conf. IMAPS XXVI*, 221–224 (2002).
5. P. Panek, M. Lipinski, R. Ciach, K. Drabczyk, and E. Bielanska, "The infrared processing in multicrystalline silicon solar cell low-cost technology", *Solar Energy Materials & Solar Cells* **76**, 529–534 (2003).
6. F. Duerinckx, J. Szlufcik, A. Ziebakowski, J. Nijs, and R. Mertens, "Simple and efficient screen printing process for multicrystalline silicon solar cells based on firing through silicon nitride", *Proc. European Photovoltaic Solar Energy Conf.* **14**, 792–795 (1997).
7. B.S. Richards, J.E. Cotter, C.B. Honsberg, and S.R. Wenham, "Novel uses of TiO_2 in crystalline silicon solar cells", *Proc. IEEE* **28**, 375–378 (2000).
8. S. Bowden, F. Duerinckx, J. Szlufcik, and J. Nijs, "Rear passivation of thin multicrystalline silicon solar cells", *Opto-Electron. Rev.* **8**, 307–310 (2000).
9. T. Zdanowicz, "The interactive computer program to fit I-V curves of solar cells", *Proc. European Photovoltaic Solar Energy Conf.* **12**, 1311–1314 (1994).
10. J. Szlufcik, F. Duerinckx, J. Horzel, E. van Kerschaver, R. Einhaus, K. De Clercq, H. Dekkers, and J. Nijs, "Advanced concept of industrial technologies of crystalline silicon solar cells", *Opto-Electron. Rev.* **8**, 299–306 (2000).
11. Information in "News" of *Renewable Energy World* **8**, 12 (2003).

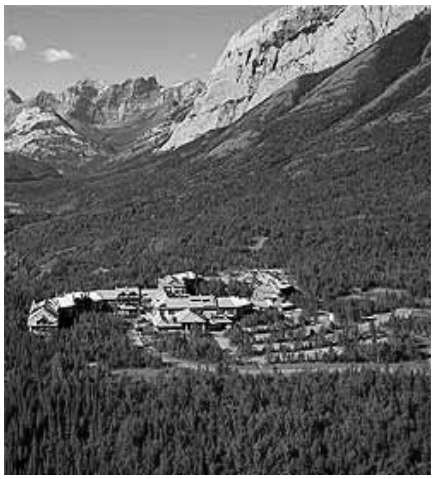

QWIP2004
International Workshop on Quantum Well Infrared Photodetectors

August 9–12, 2004
The Canadian Rockies
Delta Lodge at Kananaskis, Alberta

Chair: H.C.Liu
Co-chairs: S.D.Gunapala & H.Schneider

Advisory committee:
- Sumith Bandara – JPL USA
- Pallab Bhattacharya – U. Michigan USA
- Ph. Bois – Thales France
- Gail Brown – AFRL USA
- Anna Carbone – Polito Italy
- Dave Cardimona – AFRL USA
- E. Finkman – Technion Israel
- Bernhard Hirschauer – Acreo Sweden
- Vincent Larochelle – DRDC Canada
- Paul LeVan – AFRL USA
- Barbara McQuiston – QWIPTech USA
- Unil Perera – GSU USA
- Gabby Sarusi – Elop Israel
- Meimei Tidrow – BMDO USA
- Benny Toomarian – JPL USA

Workshop coordinator:
Tania Oogarah, Tel: 613 993–7116,
Fax: 613 990 0202,
E-mail: Tania.Oogarah@nrc.ca

Introduction:
This workshop is the third one of the series following QWIP2000 in Dana Point (USA) and QWIP2002 in Torino (Italy). QWIP is now a technology for infrared imaging, after rapid development in the past 15 years. It is also because of this rapid advance, some areas are not yet completely resolved and potentials are not fully exploited. The primary goal of this workshop is to gather all the experts in the QWIP R&D, government sponsors, industrial engineers, instrument technologists, end users, etc., and then discuss the current issues, formulate directions, and establish collaborations.

Scope:
- QWIP physics; for example, advanced or fully quantum mechanical QWIP model, realistic grating and optical coupler model, solutions to the slow response in low temperature and low background
- QWIP technology, for example, multicolor and multiband arrays
- QWIP applications, for example, military, medical/health, and commercial
- QWIP novel direction, for example, ultrahigh speed, two-photon response
- Related new approaches, for example quantum dots and other materials
- Related devices

Format:
The workshop is intended to provide a forum where ample time is allotted for presentation and discussion. The number of participants is limited to facilitate this goal. A good/basic prior knowledge of QWIP is assumed.

Tentative dates:
Abstract deadline: April 23, 2004
Notification of acceptance/rejection: May 14, 2004
Registration: June 23, 2004

